JCI insight

PD-1 blockade counteracts post-COVID-19 immune abnormalities and stimulates the anti-SARS-CoV-2 immune response

Cristian Loretelli, … , Stefano Rusconi, Paolo Fiorina

JCI Insight. 2021. https://doi.org/10.1172/jci.insight.146701.

Research In-Press Preview COVID-19 Immunology

Graphical abstract

PD-1 blockade counteracts post-COVID-19 immune abnormalities and stimulates the anti-SARS-CoV-2 immune response

Cristian Loretelli[1], Ahmed Abdelsalam[1], Francesca D'Addio[1], Moufida Ben Nasr[1,2], Emma Assi[1], Vera Usuelli[1], Anna Maestroni[1], Andy Joe Seelam[1], Elio Ippolito[1], Stefania Di Maggio[1], Lara Loreggian[1], Dejan Radovanovic[3], Claudia Vanetti[4], Jun Yang[5], Basset El Essawy[6,7], Antonio Rossi[8], Ida Pastore[8], Laura Montefusco[8], Maria Elena Lunati[8], Andrea Bolla[8], Mara Biasin[4], Spinello Antinori[4,9], Pierachille Santus[3,4], Agostino Riva[4,10], Gian Vincenzo Zuccotti[11,12], Massimo Galli[4,10], Stefano Rusconi[4,13] and Paolo Fiorina[1,2,8]

[1]International Center for T1D, Centro di Ricerca Pediatrica Romeo ed Enrica Invernizzi, Dipartimento di Scienze Biomediche e Cliniche "L. Sacco", Università di Milano, Milan, Italy; [2]Nephrology Division, Boston Children's Hospital, Harvard Medical School, Boston, MA, USA; [3]Division of Respiratory Diseases, ASST Fatebenefratelli Sacco, Milan, Italy; [4]Dipartimento di Scienze Biomediche e Cliniche "L. Sacco", Università di Milano, Milan, Italy, [5]Institute of Organ Transplantation, Tongji Hospital and Medical College, Huazhong University of Science and Technology, Wuhan, China; [6]Medicine, Al-Azhar University, Cairo, Egypt; [7]Transplantation Research Center, Nephrology Division, Brigham and Women's Hospital, Boston, MA, USA; [8]Endocrinology Division, ASST Fatebenefratelli Sacco, Milan, Italy; [9]Division of Tropical Diseases, ASST Fatebenefratelli Sacco, Milan, Italy, [10]Division of Infectious Diseases, ASST Fatebenefratelli Sacco, Milan, Italy; [11]Centro di Ricerca Pediatrica Romeo ed Enrica Invernizzi, Dipartimento di Scienze Biomediche e Cliniche "L. Sacco", Università di Milano, Milan, Italy; [12]Dipartimento di Pediatria, Ospedale dei Bambini Buzzi, Milan, Italy; [13]Infectious Diseases Unit, Legnano General Hospital, ASST Ovest Milanese, Legnano, Italy

Abstract word count: 198
Text word count: 7185
Tables/Figures: 7
Running title: PD-1 blockade and COVID-19
Keywords: SARS-CoV-2, COVID-19, Post-COVID-19, Long COVID, PD-1 blockade, immune checkpoint blockade

Address for correspondence:
Paolo Fiorina, MD PhD
Nephrology Division,
Boston Children's Hospital, Harvard Medical School
300 Longwood Ave. Enders Building
Boston MA 02115
Tel. +1 617 416 2791
E-mail: paolo.fiorina@childrens.harvard.edu

Conflict of interest statement
The authors have declared that no conflict of interest exists.

Abstract

A substantial proportion of patients who have recovered from coronavirus disease-2019 (COVID-19) experience COVID-19-related symptoms, even months after hospital discharge. We extensively immunologically characterized patients who recovered from COVID-19. In these patients, T cells were exhausted, with increased PD-1^{+} T cells, as compared to healthy controls. Plasma levels of IL-1ß, IL-1RA and IL-8, among others, were also increased in patients who recovered from COVID-19. This altered immunophenotype was mirrored by a reduced ex vivo T cell response to both nonspecific and specific stimulation, revealing a dysfunctional status of T cells, including a poor response to SARS-CoV-2 antigens. Altered levels of plasma soluble PD-L1 as well as of *PD1* promoter methylation and *PD1*-targeting miR-15-5p in CD8^{+} T cells were also observed, suggesting abnormal function of the PD-1/PD-L1 immune checkpoint axis. Notably, ex vivo blockade of PD-1 nearly normalized the aforementioned immunophenotype and restored T cell function, reverting the observed post-COVID-19 immune abnormalities; indeed, we also noted an increased T cell-mediated response to SARS-CoV-2 peptides. Finally, in a neutralization assay, PD-1 blockade did not alter the ability of T cells to neutralize SARS-CoV-2 spike pseudotyped lentivirus infection. Immune checkpoint blockade ameliorates post-COVID-19 immune abnormalities and stimulates an anti-SARS-CoV-2 immune response.

68 **Introduction**

69 A large proportion of patients discharged after being hospitalized for COVID-19 experience the
70 persistence of COVID-19-related symptoms (1-5), a condition defined as "long COVID" (6).
71 During the acute phase of COVID-19, a variety of immune alterations are evident, including
72 lymphopenia and proinflammatory cytokine storm (7-14). These immune disorders denote a broad
73 functional impairment occurring in both the innate and adaptive compartments of the immune
74 system, that may also affect the ability to counteract SARS-CoV-2 infection. Interestingly,
75 increasing evidence suggests that phenotypic and functional alterations of the immune system
76 persist long after recovery from COVID-19 (15-17). These immune abnormalities may dampen an
77 efficient immune response against viral reinfections, and may overall impair the ability to fight
78 pathogens (18-20). The urgent need for an effective cure for COVID-19 has prompted the use of
79 therapeutic strategies and accelerated the development of effective vaccines (21-37). Indeed, the
80 success of widespread vaccination has been associated with reduced hospitalization and reinfection.
81 (36, 37). Designing pharmacological strategies to stimulate the immune system may be a valuable
82 tool to abrogate or reduce over time the long-term sequelae of COVID-19-related symptoms. In this
83 report, we characterize the immune profile of patients who eventually recovered form COVID-19
84 and describe a novel strategy capable of reverting the extensive immune abnormalities observed;
85 indeed, we also noted a PD1-blockade dependent enhancement of anti-SARS-CoV-2 immune
86 response. A method to elicit a successful reversal of post-COVID-19 immune abnormalities may be
87 necessary as long term COVID-19 symptoms cause in some cases serious afflictions, and this
88 strategy could therefore be significantly clinically relevant.

Results

Immune signature of patients who recovered from COVID-19

With the aim of providing a comprehensive description of the immune signature of patients who recovered from COVID-19, we first conducted an extensive immunophenotyping analysis of cells obtained from healthy controls and patients, whose main clinical characteristics are reported in Table 1. Among lymphocytes, $CD19^+$ B cells were slightly decreased in patients who recovered from COVID-19 as compared to healthy controls, while an increase in $CD8^+$ T cells was evident in patients who recovered from COVID-19 as compared both to those in the acute phase and to healthy controls (Supplemental Figure S1A). Patients who recovered from COVID-19 also showed a higher proportion of effector $CD8^+$ T cells ($CD45RO^-CD62L^-$), while memory T cells, either effector or central ($CD45RO^+CD62L^-$ or $CD45RO^+CD62L^+$), were slightly altered among groups (Supplemental Figure S1, A and B). Furthermore, while the proportion of CD40L-expressing $CD4^+$ T cells and that of ICOS-expressing $CD8^+$ T cells was decreased in patients who recovered from COVID-19 as compared to patients with COVID-19 (Table 2), the fraction of OX40- and GITR-positive $CD8^+$ T cells of patients who recovered from COVID-19 exceeded that of healthy controls, with the latter marker being the highest observed among all groups (Table 2).

In the evaluation of exhaustion markers, $CD127^+$ and PD-1^+ $CD4^+$ T cell subpopulations were increased in patients who recovered from COVID-19 as compared to healthy controls, and were at comparable levels to those observed in patients with COVID-19 (Figure 1, A-D), while $2B4^+$ $CD4^+$ T cell levels were similar to that of healthy controls but higher compared to patients with COVID-19 (Figure 1, E and F). Furthermore, an increased fraction of cells expressing LAG3 as well as a decreased proportion of cells marked by the expression of TIGIT was observed in the $CD4^+$ T cell population of patients who recovered from COVID-19 as compared to patients with COVID-19 and to healthy controls, respectively (Figure 1, G and H), suggesting the persistence of an abnormal exhaustion profile even after symptom remission. This was further confirmed in $CD8^+$ T cells, in which several markers were upregulated in patients who recovered from COVID-19 as compared to

115 healthy controls, and/or to patients with COVID-19 (Table 2). Finally, transcriptomic profiling
116 revealed an altered pattern of $CD4^+$ and $CD8^+$ T cell gene expression in patients who recovered
117 from COVID-19 that particularly affected the $CD4^+$ T cell subpopulation, with less dysregulation
118 observed in $CD8^+$ T cells (Figure 1, I and J). Indeed, downregulation of several pro-inflammatory
119 genes, including *CSF1*, *LAT*, *LTA*, *BTLA*, *CD40LG*, *JAK1, TNFSF14* and *TNFRSF9*, was evident in
120 $CD4^+$ T cells of patients who recovered from COVID-19 as compared to healthy controls (Figure
121 1I), with *LAT* and *BTLA* also downregulated in $CD8^+$ T cells (Figure 1J). Furthermore, expression
122 levels of genes controlling cell proliferation and apoptosis, such as *TGFB1*, *CDK4*, *TNFSF10* and
123 *TNFRSF10A*, were also found to be dysregulated in $CD4^+$ T cells of patients who recovered from
124 COVID-19 (Figure 1I). Overall, these results reveal unique features in the immunophenotype of
125 patients who recovered from COVID-19.

126 ***T cell overstimulation is associated with an abnormal secretome***

127 To characterize the cytokine signature of patients who recovered from COVID-19, we assessed
128 plasma levels of a panel of 27 cytokines in subjects of the three groups using a multiplex Luminex-
129 based system (Figure 2A and Supplemental Table S1). We found that plasma levels of cytokines
130 IL-1β, IL-1RA, IL-7, IL-8, IL-10, IFN-γ and MIP-1α were higher in patients who recovered from
131 COVID-19 as compared to healthy controls, and at comparable levels to those observed in patients
132 with COVID-19 (Figure 2A), indicating a failure to return to physiological cytokine levels after
133 COVID-19. Intriguingly, levels of IL-9, eotaxin, MIP-1β and RANTES in patients who recovered
134 from COVID-19 were found to be the lowest among the three groups (Figure 2A), further
135 indicating that cytokine levels are dysregulated in patients with COVID-19 after clinical symptom
136 remission. To provide mechanistic insight into the relation between systemic release of pro-
137 inflammatory factors and the abnormal immunological phenotype observed in T cells of patients
138 with COVID-19, we exposed PBMCs isolated from healthy controls to several pro-inflammatory
139 cytokines which were increased in patients' circulation during and after COVID-19. PBMCs were
140 cultured for 48 hours in medium supplemented with human serum and containing recombinant IL-

141 1β, IL-1RA, IL-6, IL-8 and IP-10 added either individually or as a pool, after which cells were
142 collected for exhaustion and co-stimulatory marker analysis by flow cytometry. We found that
143 recombinant IP-10 administration increased the fraction of $CD4^+$ T cells that were positive for the
144 LAG3 exhaustion marker, while a lower percentage of $2B4^+$ cytotoxic $CD8^+$ T cells was detected in
145 PBMCs cultured in medium containing recombinant IL-1β or IL-6 as compared to medium alone
146 (Figure 2B and Supplemental Figure S2, A-C). To further investigate the role of these cytokines on
147 T cell phenotype, we also exposed PBMCs isolated from patients with COVID-19 to medium
148 containing their own serum in the presence of blocking antibodies directed against IL-1β, IL-1RA,
149 IL-6, IL-8 or IP-10, added either individually or as a pool. We then assessed the resultant changes
150 on expression of T cell exhaustion and activation markers by flow cytometry. PBMCs exposed to a
151 pool of sera obtained from patients with COVID-19 increased the proportion of several exhaustion
152 and costimulatory markers (Figure 2C and Supplemental Figure S3, A and B). Notably, we
153 observed an overall reversal of the COVID-19 serum-induced increase in costimulatory and
154 exhaustion marker expression on both $CD4^+$ and $CD8^+$ T cells following addition of blocking
155 antibodies to cell cultures (Figure 2C and Supplemental Figure S3, A and B). In particular, the
156 expression of PD-1 and ICOS on $CD4^+$ T cells and that of CD127 and CD40L on $CD8^+$ T cells
157 showed a marked decrease when the majority of blocking antibodies were added, both individually
158 and as a pool, to PBMCs cultured with serum obtained from patients with COVID-19 (Figure 2C
159 and Supplemental Figure S3, A and B). Overall, these findings suggest that high levels of serum
160 cytokines at least in part account for the T cell exhaustion observed in patients who recovered from
161 COVID-19.

162 ***T cells from patients who recovered from COVID-19 are dysfunctional***

163 Given the persistent T cell activation/exhaustion observed in patients who recovered from COVID-
164 19, we aimed to investigate the $CD4^+$ T cell-dependent response following specific or nonspecific
165 in vitro stimulation using an ex vivo IFN-γ based ELISpot assay. PBMCs isolated from patients
166 who recovered from COVID-19, from patients with COVID-19 and from healthy controls were

167 exposed in vitro to lipopolysaccharide (LPS), diphtheria/tetanus/pertussis vaccine (DTaP) or
168 quadrivalent flu vaccine (FLU), and the T cell-mediated response was evaluated in terms of number
169 of IFN-γ-secreting cells as indicated by the number of spots observed per 10^6 plated PBMCs
170 (Figure 3, A-F). Cells isolated from patients who recovered from COVID-19 showed a markedly
171 decreased response to nonspecific stimulation as compared to healthy controls, which resembled
172 that of patients with COVID-19 (LPS; Figure 3, A and B), and which represents an additional
173 immunological feature that distinguishes patients who have recovered from COVID-19. Given the
174 increase in PD-1-expressing T cells observed in patients who recovered from COVID-19 and the
175 role of the PD-1/PD-L1 axis in exhaustion onset, we sought to further confirm dysregulation of the
176 PD-1/PD-L1 pathway in COVID-19. We thus assessed plasma levels of soluble PD-1 (sPD-1) and
177 PD-1 ligand PD-L1 (sPD-L1), as well as the expression of PD-1- and PD-L1-targeting miRNAs
178 miR-138-5p, miR-15a-5p, miR-16-5p and miR-28-5p in $CD4^+$ and $CD8^+$ T cells, and the extent of
179 *PD1* promoter DNA methylation in $CD4^+$/$CD8^+$ T cells isolated from patients who recovered from
180 COVID-19 as compared to those with COVID-19 and healthy controls (Figure 3, G-M).
181 Interestingly, we found lower serum sPD-L1 levels in patients who recovered from COVID-19 as
182 compared to both healthy controls and patients with COVID-19 (Figure 3H), suggesting an
183 overstimulation of the PD-1/PD-L1 axis in these patients. This conclusion was further supported
184 when we compared the PBMC-specific response to DTaP antigen stimulation in patients with
185 higher (above the median) versus lower (below the median) plasma sPD-1 or sPD-L1 levels. High
186 levels of both sPD-1 and sPD-L1 were associated with a marked decrease in the PBMC immune
187 response to DTaP in patients who recovered from COVID-19 and patients with COVID-19 as
188 compared to healthy controls (Figure 3, I and J). We next investigated the methylation status of a
189 specific *PD1* promoter CpG site that is reported to control *PD1* gene expression in $CD4^+$ and $CD8^+$
190 T cells. Methylation-specific qPCR results demonstrated an altered degree of *PD1* promoter
191 methylation in $CD8^+$ T cells – but not in $CD4^+$ T cells – of subjects who recovered from COVID-19
192 as compared to healthy controls, confirming dysregulation of the PD-1/PD-L1 axis in patients who

193 recovered from COVID-19 (Figure 3L). In $CD8^+$ T cells – but not in $CD4^+$ T cells – the PD-1
194 miRnet was also found to be altered, as shown by the higher expression of miR-15a-5p in patients
195 who recovered from COVID-19 and in patients with COVID-19 as compared to healthy controls
196 (Figure 3M). Overall, our results suggest an abnormal T cell phenotype and function of the immune
197 response in patients who recovered from COVID-19 (Figure 3N), which is at least partially due to a
198 dysregulated PD-1/PD-L1 axis in T cells. Interestingly, these immune abnormalities were found to
199 be associated with a persistence of dyspnea and several additional COVID-19-related symptoms at
200 time of recruitment (Table 3).

201 **In vitro *PD-1 blockade restores T cell function***

202 Based on these results, we hypothesized that PD-1 blockade could counteract post-COVID-19
203 immune abnormalities (Figure 4A). We therefore sought to determine whether PD-1 blockade,
204 achieved by use of a clinically relevant anti-PD-1 blocking monoclonal antibody (mAb), would
205 revert the exhaustion status of T cells and restore their functional activity in response to specific and
206 nonspecific stimulation. In an ELISpot ex vivo assay, we examined the function of T cells in
207 patients who recovered from COVID-19 and in controls following challenge with LPS, DTaP and
208 FLU in the presence of anti-PD-1 mAb. FLU-stimulated PBMCs collected from patients who
209 recovered from COVID-19 and cultured in the presence of anti-PD-1 displayed a significantly
210 enhanced immune response as compared to FLU-only-stimulated PBMCs (Figure 4B). A similar
211 pattern was observed when using PBMCs from healthy controls, in which cells cultured with anti-
212 PD-1 mAb showed an increased response to DTaP stimulation as compared to DTaP-only-treated
213 cells (Figure 4B). Given the increased expression of costimulatory and exhaustion T cell markers
214 observed in patients who recovered from COVID-19, we next investigated the ability of PD-1
215 blockade to reverse this phenotype (Figure 4, C-J and Supplemental Figure S4, A and B). Ex vivo
216 anti-PD-1 blockade reversed the increase in the expression of the positive costimulatory marker
217 OX40 in the $CD8^+$ T cell fraction that was observed in patients who recovered from COVID-19
218 (Figure 4E). Moreover, PD-1 blockade in PBMCs isolated from patients with COVID-19 resulted in

219 a decrease in the percentage of exhausted T cells (Figure 4, C-J). Taken together, our data indicate
220 that in T cells isolated from patients with COVID-19 upon PD-1 immune checkpoint blockade, T
221 cell immune response and phenotype improve. We then examined in an ex vivo assay the T cell
222 response to a pool of peptides derived from SARS-CoV-2 spike and nucleocapsid proteins, with or
223 without the administration of anti-PD-1 blocking mAb, or in the presence of an anti-human IgG
224 used as a negative control. The number of IFN-γ-producing cells was then quantified in an ELISpot
225 assay. A sizeable T cell response against SARS-CoV-2 antigens at baseline was mounted only when
226 PBMCs isolated from patients who recovered from COVID-19 were used (Figure 4K). Remarkably,
227 the addition of anti-PD-1 mAb resulted in a two-fold increase in the number of IFN-γ-producing
228 cells as compared to SARS-CoV-2 peptide-only treated cells or to the negative control (Figure 4K).
229 This finding confirms that PD-1 blockade is able to bolster the specific T cell immune response to
230 SARS-CoV-2 antigens, thus reinstating their functional activation. We then verified if PD-1
231 blockade prevents T lymphocyte-mediated neutralization of SARS-CoV-2 virus. To this aim, we
232 developed a SARS-CoV-2 cell-based neutralization assay to indirectly assess the $CD3^+$ T cell
233 antiviral response. First, a SARS-CoV-2 spike pseudotyped lentivirus containing a luciferase
234 reporter gene was exposed to $CD3^+$ T cells isolated from patients who recovered from COVID-19
235 in the presence of anti-PD-1 blocking antibody. Residual pseudoviral particles were collected and
236 used to infect SARS-CoV-2 infection-sensitive, ACE2-overexpressing 293T cells, and T
237 lymphocyte neutralization activity was measured by comparing luciferase activity in infected cells
238 (Figure 4L). The sera of patients who recovered from COVID-19 containing high titers of anti-
239 SARS-CoV-2 IgG was used as a positive control. Lymphocyte-driven pseudovirus neutralization
240 was observed when pseudoviral particles were exposed to $CD3^+$ T cells of patients who recovered
241 from COVID-19 upon PD-1 blockade, in a comparable pattern to that which was observed when
242 sera of patients who recovered from COVID-19 was used (Figure 4L). We thus demonstrate that
243 PD-1 blockade enhances the anti-SARS-CoV-2 specific immune response and reinforces PBMC-
244 mediated SARS-CoV-2 anti-viral activity.

245 **Discussion**

246 The longitudinal dynamics of the immune response following COVID-19 has gathered attention,
247 primarily because of its implications regarding the existence of long-term health concerns (7, 38-
248 41). In this report, we have performed a comprehensive immunophenotypic and functional profiling
249 of patients who have recovered from COVID-19. Our findings have enabled the identification and
250 characterization of a panel of immunological parameters, the dysregulation of which persists after
251 COVID-19-related symptom remission. Patients who recovered from COVID-19 show alterations
252 in the proportion of immune cell subsets, including cytotoxic $CD8^+$ T cells as well as effector and
253 effector memory T cells. The functional phenotype of T cells in these patients is also abnormal,
254 displaying higher expression of several costimulatory and exhaustion T cell markers, including PD-
255 1. These findings confirmed previously observations of a deranged immune profile in patients
256 recovered from COVID-19 (15-17). According to our data, such functional imbalance is reflected at
257 the transcriptional level by altered mRNA expression of several genes involved in T cell activation
258 (*CSF1*, *LAT*, *LTA*, *CD40LG*, *JAK1*), modulation (*BTLA*), proliferation (*CDK4*) and apoptosis
259 (*TGFB1*, *CDK4*, *TNFSF10* and *TNFRSF10A*), highlighting the persistence of perturbation of T cell
260 function after clinical remission from COVID-19. We also observed substantially higher amounts of
261 several relevant cytokines, including IL-1ß, IL-1RA and IL-8, which were not restored to normal
262 levels after resolution of the acute phase of the disease. The dysregulated functional phenotype
263 observed in patients who recovered from COVID-19 may be at least partially linked to the
264 abnormal systemic cytokine levels characterizing a cytokine storm, since PBMCs isolated from
265 healthy controls and exposed to recombinant IL-1β, IL-6 or IP-10 are subject to altered expression
266 of LAG3 and 2B4, while antibody-mediated blockade of different cytokines – including IL-1β, IL-
267 1RA, IL-6, IL-8 and IP-10 – promotes reversal of the COVID-19 serum-induced increase in
268 exhaustion and costimulatory markers observed in both $CD4^+$ and $CD8^+$ T cells. Overall, these
269 findings reveal unique and abnormal features of the immunophenotype of patients who have
270 recovered from COVID-19. T cells of patients who recovered from COVID-19 are unresponsive

271 when challenged ex vivo with both specific (DTaP) and nonspecific (LPA) stimulations, and this
272 failure to respond is accompanied by a higher fraction of PD-1-expressing T cells. Further analyses
273 confirmed a dysfunctional PD-1/PD-L1 immune checkpoint axis in patients who recovered from
274 COVID-19, as revealed by lower plasma levels of soluble PD-L1, as well as by increased
275 expression of miR-15a-5p – a previously reported *PD1*-targeting miRNA with inhibitory effects –
276 and by higher *PD1* promoter methylation occurring in $CD8^+$ T cells as compared to healthy
277 controls. These findings are consistent with the view that the PD-1/PD-L1 axis is overstimulated in
278 T cells of patients who recovered from COVID-19. These data prompted us to test whether T cell
279 exhaustion can be reversed and whether T cell function can be restored by PD-1 blockade. Indeed,
280 the blockade of PD-1 enhanced the specific T cell-mediated response to a flu vaccine and reverted
281 the observed overstimulation/exhaustion phenotype. Interestingly, we noticed that PD-1 blockade
282 also increased the $CD4^+$ T cell-mediated response to a pool of SARS-CoV-2 spike and nucleocapsid
283 peptides, with no negative effect on lymphocyte-mediated SARS-CoV-2 anti-viral activity. In
284 patients with COVID-19, the T cell response is attenuated during the initial phases of the infection
285 (8, 10, 11, 42, 43). While most current therapeutic options for treating patients with COVID-19 are
286 directed to either contain replication of SARS-CoV-2 (21-25, 36) or to control inflammation (27-30,
287 44), a successful treatment may require a well-functioning immune system with proficient T cell
288 function. The array of post-COVID-19 immune abnormalities we reported here may embody an
289 immune weakness, which may favor COVID-19 recurrence and impair the ability to fight
290 pathogens, that can be reverted by PD-1 blockade. Anti-PD-1 blocking compounds are currently
291 successfully used as immunotherapeutic to enhance the anti-tumor immune response in cancer
292 patients (45) and is being investigated for alleviating and resolving chronic infections (46) as well
293 as autoimmune diabetes (47-49). Further future studies may support PD-1 blockade as a potential
294 tool to correct the immune abnormalities persisting after remission from COVID-19 and restore full
295 competence of the immune system. In summary, by using a broad phenotypic and functional
296 immune characterization approach, here we report that patients who recovered from COVID-19

297 present with post-COVID-19 immunological abnormalities consisting of an aberrant immune cell
298 and cytokine profile, as well as impaired T cell function even months after hospital discharge. We
299 also show that immune checkpoint PD-1 blockade reverts such immune abnormalities and restores a
300 nearly normal T cell phenotype and function. Further studies performed on murine model would be
301 ideal to ascertain the ability of in vivo PD-1 blockade to revert phenotypic and functional immune
302 alterations induced by SARS-CoV-2 infection that persist after recovery from COVID-19.

303 **Methods**

304 For a full description of the methods, please refer to the online supplemental materials.

305 ***Patients***

306 Consecutively admitted patients with COVID-19 or patients who recovered from COVID-19
307 infection admitted for SARS-CoV-2 acute infection at the Infectious Disease and Respiratory
308 Division of ASST FBF-Sacco in Milan from March 31, 2020 to October 2, 2020 were enrolled and
309 compared with a group of healthy control subjects. SARS-CoV-2 infection of all enrolled patients
310 was confirmed by viral PCR of nasal and pharyngeal swab specimens collected during the acute
311 phase of the infection, according to WHO guidance. Patient baseline clinical score was determined
312 according to a modified ordinal score based on 7 major points as previously reported (31). Baseline
313 demographic distributions, clinical, laboratory, management, and outcome data were abstracted
314 from patient electronic medical reports. Immunophenotyping was performed by flow cytometry
315 using antibodies listed in Supplemental Table S2.

316 ***ELISpot assay***

317 An ELISpot assay was used to measure the number of IFN-γ-producing cells according to the
318 manufacturer's protocol (BD Biosciences, USA) as previously shown by our group (50). For testing
319 nonspecific ex vivo T cell responses, $3x10^5$ PBMCs isolated from healthy control subjects, from
320 patients with COVID-19 and from patients who recovered from COVID-19 were cultured for 48h
321 in RPMI 1640 10% FBS in the presence of lipopolysaccharide (LPS, 1 μg/ml; Merk, USA),
322 influenza vaccine (FLU), or a trivalent diphtheria, tetanus and pertussis vaccine (DTaP), with or
323 without the addition of an anti-PD-1 blocking antibody (pembrolizumab, 5 μg/ml). At day 2 post-
324 stimulation, cells were collected and plated on a human IFN-γ ELISpot assay plate, and spots were
325 counted using an ImmunoSpot Reader (CTL Europe GmbH, Bonn, Germany). The specific
326 response to SARS-CoV-2 antigens was tested by culturing $3x10^5$ PBMCs isolated from healthy
327 control subjects, patients with COVID-19 and from patients who recovered from COVID-19 for
328 48h in RPMI 1640 10% FBS in the presence of pooled peptides derived from SARS-CoV-2 spike

329 and nucleocapsid proteins (PR-nCoV-1, PR-nCoV-3; Novatein Biosciences, USA) (1 μg/ml) with
330 or without the addition of the anti-PD-1 blocking antibody pembrolizumab (Keytruda, MSD,
331 Kenilworth, NJ, USA) (5 μg/ml) or of an anti-human IgG antibody used as a negative control
332 (Yumab, Braunschweig, Germany) (5 μg/ml). At day 2 post-stimulation, cells were collected and
333 plated using the human IFN-γ ELISpot assay and processed as previously described.

334 ***Pseudo-SARS-CoV-2 neutralization assay***

335 Spike SARS-CoV2 pseudotyped lentiviruses containing a luciferase reporter (BPS Bioscience, San
336 Diego, CA, USA) were used in our modified neutralization assay. Briefly, 5 μl of SARS-CoV-2
337 pseudotyped lentivirus were incubated with $5x10^5$ PBMCs from patients who recovered from
338 COVID-19 with the addition of anti-PD-1 blocking antibody. Cells were cultured in RPMI 1640 in
339 a 96-well white clear-bottom assay plate and incubated for 12 hours at 37° C. SARS-CoV-2
340 pseudotyped lentivirus incubated with serum collected from patients who recovered from COVID-
341 19 served as a positive control. After incubation, supernatants were collected from every condition
342 and used for infection of ACE2-overexpressing 293T cells (BPS Bioscience), then further incubated
343 for 48 hours in 5% CO_2 at 37° C. Luminescence, which is correlated to the luciferase activity on
344 293T cells, was quantified using the One-step Luciferase Assay System as recommended by the
345 manufacturer on a GloMAX luminometer (both from Promega, Madison, WI, USA).

346 ***Statistics***

347 Prism version 7.0 (GraphPad, La Jolla, CA, USA) was used as for statistical analysis and graphical
348 representation of data. The sample distribution was determined by the Shapiro-Wilk normality test.
349 One-way ANOVA, two-sided t-test or non-parametric Kruskal-Wallis and Mann-Whitney tests
350 were performed where appropriate and according to data distribution. All data are presented as
351 mean ± SEM, with p values less than 0.05 considered as significant.

352 ***Study approval***

353 All samples were obtained from patients and healthy controls after provision of informed consent
354 and in accordance with the local Ethical Research Committee of Milan (Comitato Etico Milano
355 Area 1) which granted the approval of the present study.

356 **Author contributions**

357 C.L. designed and performed experiments, analyzed data, wrote and edited the paper; A.A., F.D.,
358 M.BN., designed and performed research, analyzed the data, and edited the paper; E.A., V.U.,
359 A.M., A.J.S., E.I., S.DM., L.L., C.V. and M.B. collected and analyzed data; D. R., A.Ro., I.P., L.M.
360 M.E.L., A.B., S.A. and A.Ri. assisted with sample collection and data analysis; J.Y., B.EE., P.S.,
361 G.V.Z., S.R. and M.G. coordinated research and edited the paper; P.F. conceived the idea, designed
362 the study and wrote and edited the paper. All authors were given full access to all data presented in
363 this study and are responsible for the integrity of the data and accuracy of the data analysis. All
364 authors have given their permission for submission of this manuscript.

365

366 **Acknowledgments**

367 We thank Dr. Mollie Jurewicz for editorial assistance. We are thankful to Fondazione Romeo and
368 Enrica Invernizzi for extraordinary support.

369

370 **Funding**

371 P.F. is supported by the Italian Ministry of Health grant RF-2016-02362512. F.D. is the recipient of
372 the SID Lombardia Grant and of the EFSD/JDRF/Lilly Programme on Type 1 Diabetes Research
373 2019.

374

375 **Duality of interest**

376 All authors declare no present or potential conflicts of interest. This study was performed without
377 the support of any external funding source or study sponsor.

378 **References**

379 1. Carfi A, et al. Persistent Symptoms in Patients After Acute COVID-19. *JAMA.*
380 2020;324(6):603-5.

381 2. Nalbandian A, et al. Post-acute COVID-19 syndrome. *Nat Med.* 2021;27(4):601-15.

382 3. Chopra V, et al. Sixty-Day Outcomes Among Patients Hospitalized With COVID-19. *Ann*
383 *Intern Med.* 2021;174(4):576-8.

384 4. Huang C, et al. 6-month consequences of COVID-19 in patients discharged from hospital: a
385 cohort study. *Lancet.* 2021;397(10270):220-32.

386 5. Montefusco L, et al. Acute and long-term disruption of glycometabolic control after SARS-
387 CoV-2 infection. *Nat Metab.* 2021.

388 6. Long COVID: let patients help define long-lasting COVID symptoms. *Nature.*
389 2020;586(7828):170.

390 7. Mathew D, et al. Deep immune profiling of COVID-19 patients reveals distinct
391 immunotypes with therapeutic implications. *Science.* 2020;369(6508).

392 8. Qin C, et al. Dysregulation of Immune Response in Patients With Coronavirus 2019
393 (COVID-19) in Wuhan, China. *Clin Infect Dis.* 2020;71(15):762-8.

394 9. Huang C, et al. Clinical features of patients infected with 2019 novel coronavirus in Wuhan,
395 China. *Lancet.* 2020;395(10223):497-506.

396 10. Chen N, et al. Epidemiological and clinical characteristics of 99 cases of 2019 novel
397 coronavirus pneumonia in Wuhan, China: a descriptive study. *Lancet.*
398 2020;395(10223):507-13.

399 11. Diao B, et al. Reduction and Functional Exhaustion of T Cells in Patients With Coronavirus
400 Disease 2019 (COVID-19). *Front Immunol.* 2020;11:827.

401 12. Zheng M, et al. Functional exhaustion of antiviral lymphocytes in COVID-19 patients. *Cell*
402 *Mol Immunol.* 2020;17(5):533-5.

403 13. De Biasi S, et al. Marked T cell activation, senescence, exhaustion and skewing towards
404 TH17 in patients with COVID-19 pneumonia. *Nat Commun.* 2020;11(1):3434.
405 14. Zheng HY, et al. Elevated exhaustion levels and reduced functional diversity of T cells in
406 peripheral blood may predict severe progression in COVID-19 patients. *Cell Mol Immunol.*
407 2020;17(5):541-3.
408 15. Shuwa HA, et al. Alterations in T and B cell function persist in convalescent COVID-19
409 patients. *Med (N Y).* 2021;2(6):720-35 e4.
410 16. Szabo PA, et al. Longitudinal profiling of respiratory and systemic immune responses
411 reveals myeloid cell-driven lung inflammation in severe COVID-19. *Immunity.*
412 2021;54(4):797-814 e6.
413 17. Zhang JY, et al. Single-cell landscape of immunological responses in patients with COVID-
414 19. *Nat Immunol.* 2020;21(9):1107-18.
415 18. Li Q, et al. The Impact of Mutations in SARS-CoV-2 Spike on Viral Infectivity and
416 Antigenicity. *Cell.* 2020;182(5):1284-94 e9.
417 19. Tillett RL, et al. Genomic evidence for reinfection with SARS-CoV-2: a case study. *Lancet*
418 *Infect Dis.* 2021;21(1):52-8.
419 20. Plante JA, et al. Spike mutation D614G alters SARS-CoV-2 fitness. *Nature.*
420 2021;592(7852):116-21.
421 21. Baden LR, and Rubin EJ. Covid-19 - The Search for Effective Therapy. *N Engl J Med.*
422 2020;382(19):1851-2.
423 22. Solerte SB, et al. Dipeptidyl peptidase-4 (DPP4) inhibition in COVID-19. *Acta Diabetol.*
424 2020;57(7):779-83.
425 23. Goldman JD, et al. Remdesivir for 5 or 10 Days in Patients with Severe Covid-19. *N Engl J*
426 *Med.* 2020.
427 24. Gattinoni L, et al. COVID-19 pneumonia: different respiratory treatments for different
428 phenotypes? *Intensive Care Med.* 2020;46(6):1099-102.

429 25. Mair-Jenkins J, et al. The effectiveness of convalescent plasma and hyperimmune
430 immunoglobulin for the treatment of severe acute respiratory infections of viral etiology: a
431 systematic review and exploratory meta-analysis. *J Infect Dis.* 2015;211(1):80-90.
432 26. Wang C, et al. A human monoclonal antibody blocking SARS-CoV-2 infection. *Nat*
433 *Commun.* 2020;11(1):2251.
434 27. Luo P, et al. Tocilizumab treatment in COVID-19: A single center experience. *J Med Virol.*
435 2020;92(7):814-8.
436 28. Thachil J. The versatile heparin in COVID-19. *J Thromb Haemost.* 2020;18(5):1020-2.
437 29. Mehta P, et al. COVID-19: consider cytokine storm syndromes and immunosuppression.
438 *Lancet.* 2020;395(10229):1033-4.
439 30. Cavalli G, et al. Interleukin-1 blockade with high-dose anakinra in patients with COVID-19,
440 acute respiratory distress syndrome, and hyperinflammation: a retrospective cohort study.
441 *Lancet Rheumatol.* 2020;2(6):e325-e31.
442 31. Solerte SB, et al. Sitagliptin Treatment at the Time of Hospitalization Was Associated With
443 Reduced Mortality in Patients With Type 2 Diabetes and COVID-19: A Multicenter, Case-
444 Control, Retrospective, Observational Study. *Diabetes Care.* 2020;43(12):2999-3006.
445 32. Juul S, et al. Interventions for treatment of COVID-19: a protocol for a living systematic
446 review with network meta-analysis including individual patient data (The LIVING Project).
447 *Syst Rev.* 2020;9(1):108.
448 33. Giacomelli A, et al. Early administration of lopinavir/ritonavir plus hydroxychloroquine
449 does not alter the clinical course of SARS-CoV-2 infection: a retrospective cohort study. *J*
450 *Med Virol.* 2020.
451 34. Alhazzani W, et al. Surviving Sepsis Campaign: guidelines on the management of critically
452 ill adults with Coronavirus Disease 2019 (COVID-19). *Intensive Care Med.*
453 2020;46(5):854-87.

454 35. Russell CD, et al. Clinical evidence does not support corticosteroid treatment for 2019-
455 nCoV lung injury. *Lancet.* 2020;395(10223):473-5.
456 36. Corbett KS, et al. Evaluation of the mRNA-1273 Vaccine against SARS-CoV-2 in
457 Nonhuman Primates. *N Engl J Med.* 2020.
458 37. Folegatti PM, et al. Safety and immunogenicity of the ChAdOx1 nCoV-19 vaccine against
459 SARS-CoV-2: a preliminary report of a phase 1/2, single-blind, randomised controlled trial.
460 *Lancet.* 2020;396(10249):467-78.
461 38. Juno JA, et al. Humoral and circulating follicular helper T cell responses in recovered
462 patients with COVID-19. *Nat Med.* 2020;26(9):1428-34.
463 39. Tang F, et al. Lack of peripheral memory B cell responses in recovered patients with severe
464 acute respiratory syndrome: a six-year follow-up study. *J Immunol.* 2011;186(12):7264-8.
465 40. Robbiani DF, et al. Convergent antibody responses to SARS-CoV-2 in convalescent
466 individuals. *Nature.* 2020;584(7821):437-42.
467 41. Fadini GP, et al. Prevalence and impact of diabetes among people infected with SARS-CoV-
468 2. *J Endocrinol Invest.* 2020;43(6):867-9.
469 42. Chau AS, et al. The Longitudinal Immune Response to Coronavirus Disease 2019: Chasing
470 the Cytokine Storm. *Arthritis Rheumatol.* 2020.
471 43. Liu Z, et al. Lymphocyte subset (CD4+, CD8+) counts reflect the severity of infection and
472 predict the clinical outcomes in patients with COVID-19. *J Infect.* 2020;81(2):318-56.
473 44. Chen C, et al. Thalidomide combined with low-dose short-term glucocorticoid in the
474 treatment of critical Coronavirus Disease 2019. *Clin Transl Med.* 2020.
475 45. Syn NL, et al. De-novo and acquired resistance to immune checkpoint targeting. *Lancet*
476 *Oncol.* 2017;18(12):e731-e41.
477 46. Barber DL, et al. Restoring function in exhausted CD8 T cells during chronic viral infection.
478 *Nature.* 2006;439(7077):682-7.

479 47. Ben Nasr M, et al. PD-L1 genetic overexpression or pharmacological restoration in
480 hematopoietic stem and progenitor cells reverses autoimmune diabetes. *Sci Transl Med.*
481 2017;9(416).
482 48. Ben Nasr M, et al. Prostaglandin E2 Stimulates the Expansion of Regulatory Hematopoietic
483 Stem and Progenitor Cells in Type 1 Diabetes. *Front Immunol.* 2018;9:1387.
484 49. Guleria I, et al. Mechanisms of PDL1-mediated regulation of autoimmune diabetes. *Clin*
485 *Immunol.* 2007;125(1):16-25.
486 50. Petrelli A, et al. IL-21 is an antitolerogenic cytokine of the late-phase alloimmune response.
487 *Diabetes.* 2011;60(12):3223-34.

488 **Figures**

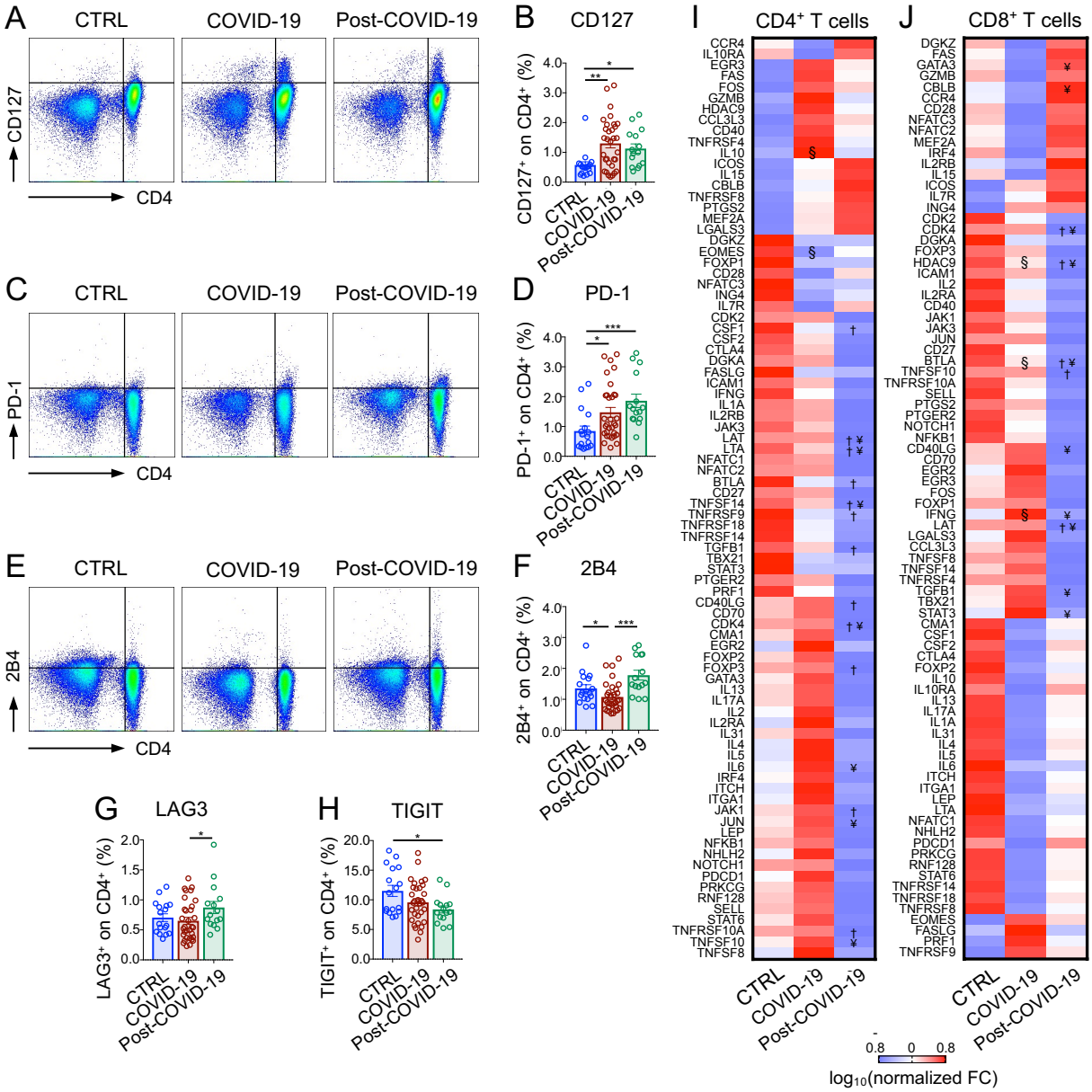

489

490 **Figure 1**. **Immune signature of patients with COVID-19 and post-COVID-19 as compared to**
491 **healthy controls**. **(A-H).** Dot plot representations (**A**, **C**, **E**) and bar graphs (**B**, **D**, **F-H**) depicting
492 the percentage of CD127$^+$, PD-1$^+$, 2B4$^+$, LAG3$^+$ and TIGIT$^+$ CD4$^+$ T cells as assessed by flow
493 cytometric analysis in the same patient groups. **(I-J).** Heatmap representation of exhaustion marker
494 transcriptomic profiling of isolated CD4$^+$ (**I**) and CD8$^+$ (**J**) T cells isolated from patients with
495 COVID-19 (n=3), from those who recovered from COVID-19 (n=3) and in healthy controls (n=3).
496 Data in all panels are reported as mean ± standard error (SEM), unless otherwise reported. (§):
497 COVID-19 vs. CTRL; (†): Post-COVID-19 vs. CTRL; (¥): Post-COVID-19 vs. COVID-19;

498 *p<0.05, **p<0.01, ***p<0.001 calculated with Kruskal-Wallis test (**B**, **D**, **F-H**) or with Spearman

499 rank correlation method (**I-J**).

500 **Abbreviations**: CTRL, healthy controls; COVID-19, patients with COVID-19; Post-COVID-19,

501 patients who recovered from COVID-19; FC, fold change.

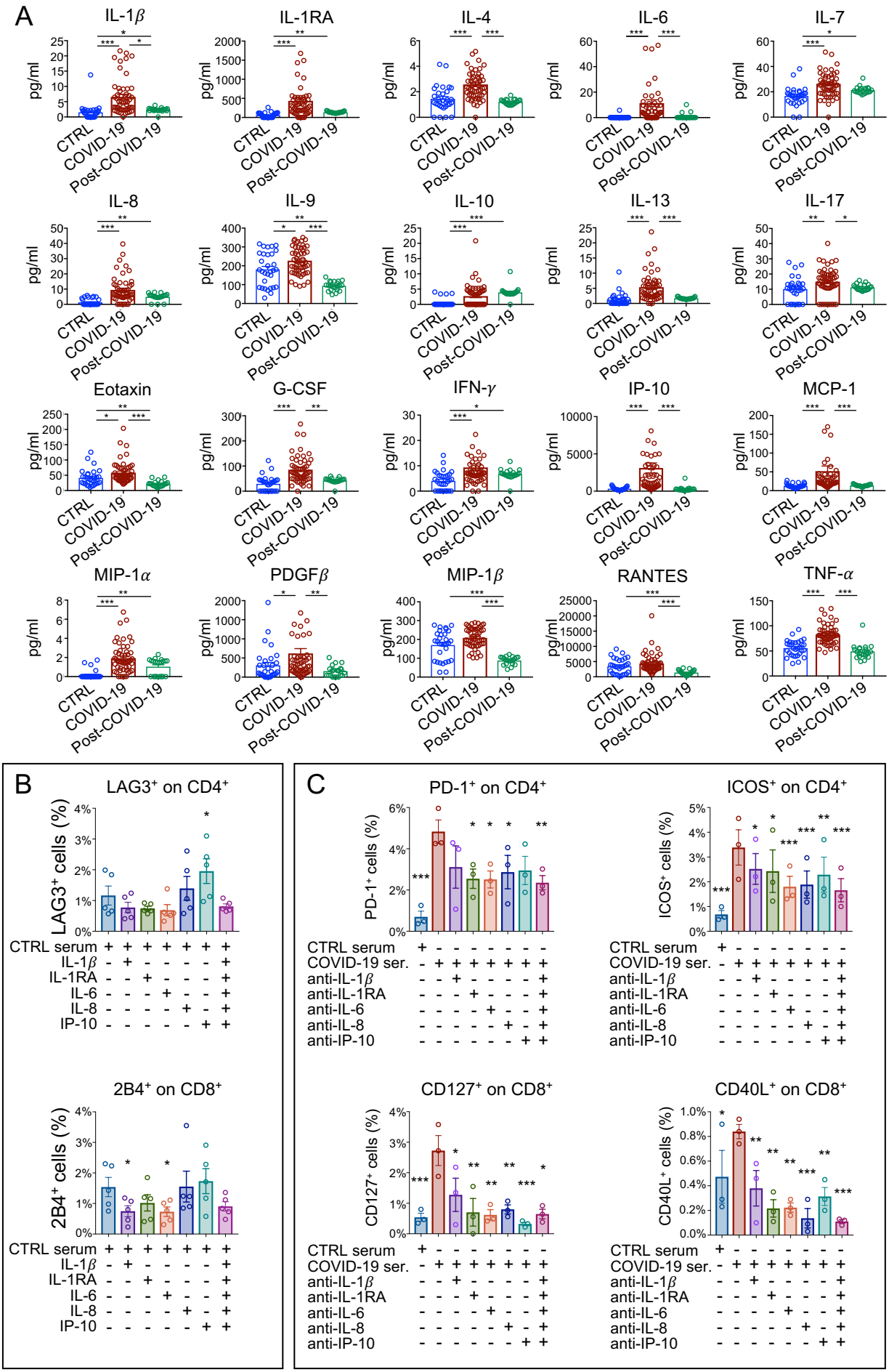
A
IL-1β
IL-1RA
IL-4
IL-6
IL-7
IL-8
IL-9
IL-10
IL-13
IL-17
Eotaxin
G-CSF
IFN-γ
IP-10
MCP-1
MIP-1α
PDGFβ
MIP-1β
RANTES
TNF-α
pg/ml
CTRL
COVID-19
Post-COVID-19
B
LAG3+ on CD4+
LAG3+ cells (%)
2B4+ on CD8+
2B4+ cells (%)
CTRL serum
IL-1β
IL-1RA
IL-6
IL-8
IP-10
C
PD-1+ on CD4+
PD-1+ cells (%)
ICOS+ on CD4+
ICOS+ cells (%)
CD127+ on CD8+
CD127+ cells (%)
CD40L+ on CD8+
CD40L+ cells (%)
CTRL serum
COVID-19 ser.
anti-IL-1β
anti-IL-1RA
anti-IL-6
anti-IL-8
anti-IP-10

502

503 **Figure 2. Cytokine profile and T cell exhaustion in patients who recovered from COVID-19 as**
504 **compared to those with COVID-19 and to healthy controls**. **(A)**. Bar graphs depicting cytokine
505 serum levels assessed by Luminex-based technology in patients with COVID-19 (n=50), in those
506 who recovered from COVID-19 (n=20) and in healthy controls (n=30). **(B)**. Bar graphs depicting
507 the percentage of $LAG3^+$ cells in the $CD4^+$ T cell population and of $2B4^+$ cells in $CD8^+$ T cells
508 assessed by flow cytometric analysis in PBMCs of healthy controls (n=5) that were treated ex vivo
509 with selected proinflammatory cytokines, either individually or as a pool. **(C)**. Bar graph depicting
510 percentage of $PD\text{-}1^+$ and $ICOS^+$ $CD4^+$ T cells and of $CD127^+$ and $CD40L^+$ $CD8^+$ T cells as assessed
511 by flow cytometric analysis of PBMCs isolated from patients with COVID-19 (n=5) that were
512 exposed ex vivo to medium containing serum of patients with COVID-19 in the presence of
513 blocking antibodies directed against IL-1β, IL-1RA, IL-6, IL-8 or IP-10, added either individually
514 or as a pool. Data are reported as mean ± standard error (SEM) unless otherwise reported. *$p<0.05$,
515 **$p<0.01$, ***$p<0.001$ calculated with Kruskal-Wallis test (**A**) or one-way ANOVA (**B-C**).
516 **Abbreviations:** CTRL, healthy controls; COVID-19, patients with COVID-19; Post-COVID-19,
517 patients who recovered from COVID-19; PBMCs, peripheral blood mononuclear cells.

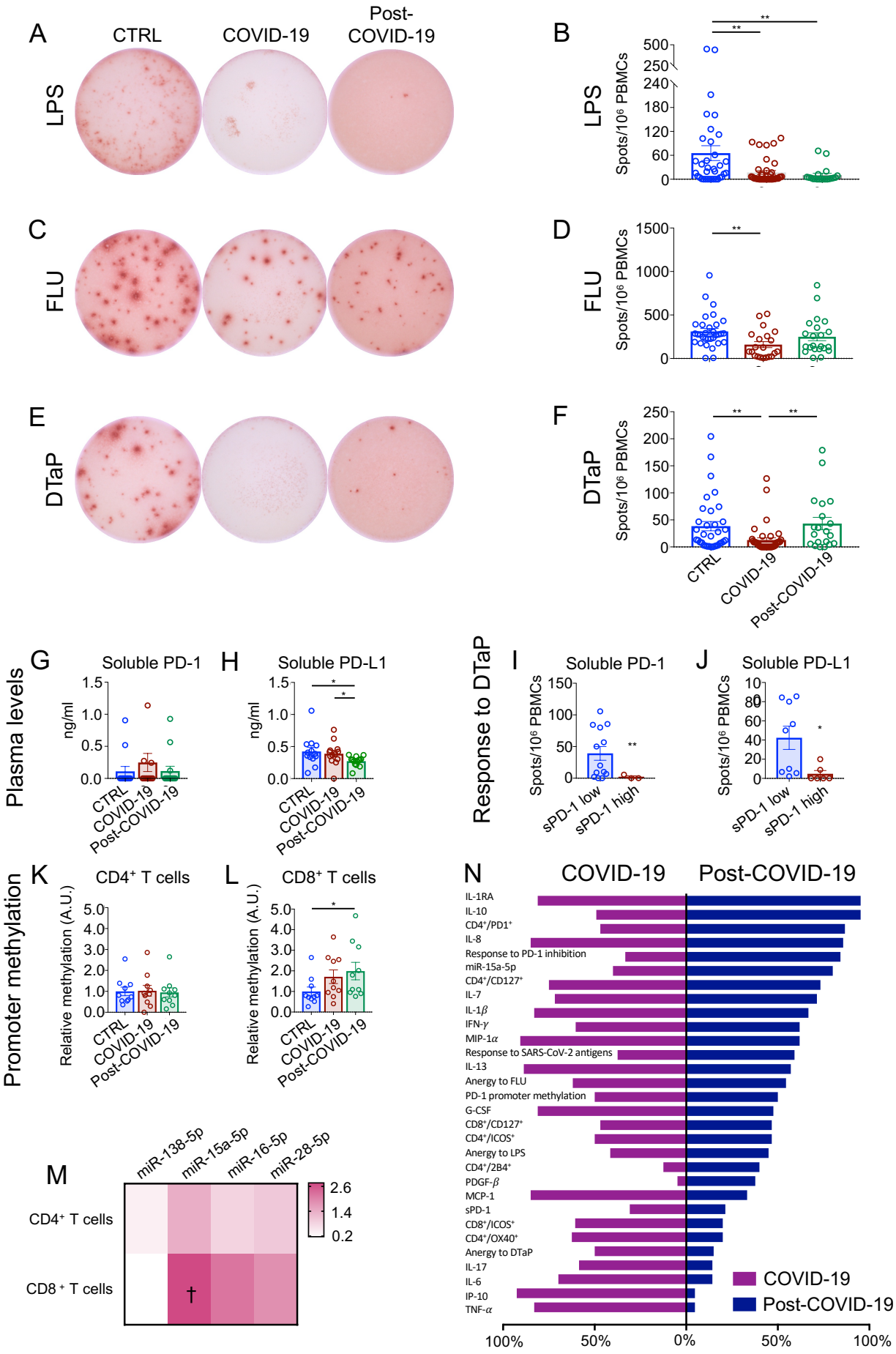
A
CTRL
COVID-19
Post-COVID-19
LPS
B
LPS
Spots/10⁶ PBMCs
C
FLU
D
FLU
E
DTaP
F
DTaP
CTRL
COVID-19
Post-COVID-19
Plasma levels
G
Soluble PD-1
H
Soluble PD-L1
ng/ml
Response to DTaP
I
Soluble PD-1
J
Soluble PD-L1
sPD-1 low
sPD-1 high
Promoter methylation
K
CD4⁺ T cells
L
CD8⁺ T cells
Relative methylation (A.U.)
M
miR-138-5p
miR-15a-5p
miR-16-5p
miR-28-5p
CD4⁺ T cells
CD8⁺ T cells
N
COVID-19
Post-COVID-19
IL-1RA
IL-10
CD4⁺/PD1⁺
IL-8
Response to PD-1 inhibition
miR-15a-5p
CD4⁺/CD127⁺
IL-7
IL-1β
IFN-γ
MIP-1α
Response to SARS-CoV-2 antigens
IL-13
Anergy to FLU
PD-1 promoter methylation
G-CSF
CD8⁺/CD127⁺
CD4⁺/ICOS⁺
Anergy to LPS
CD4⁺/2B4⁺
PDGF-β
MCP-1
sPD-1
CD8⁺/ICOS⁺
CD4⁺/OX40⁺
Anergy to DTaP
IL-17
IL-6
IP-10
TNF-α
100%
50%
0%
50%
100%

518

519 **Figure 3. T cells from patients who recovered from COVID-19 are exhausted. (A-F).**
520 Representative images and bar graphs of ELISpot analysis depicting IFN-γ spots produced by
521 PBMCs isolated from patients with COVID-19 (n=40), from those who recovered from COVID-19
522 (n=20) and from healthy controls (n=30) following challenge with LPS (A-B), FLU (C-D), and
523 DTaP (E-F). **(G-H).** Bar graphs depicting soluble PD-1 and soluble PD-L1 plasma levels in patients
524 with COVID-19 (n=13), in those who recovered from COVID-19 (n=13) and in healthy controls
525 (n=14). **(I-J).** Bar graphs depicting the immune T cell response upon DTaP stimulation in patients
526 with COVID-19 with high (above the median) versus low (below the median) levels of soluble PD-
527 1 (I) or PD-L1 (J). (**K-L**) Relative levels of *PD-1* promoter DNA methylation in $CD4^+$ (K) or $CD8^+$
528 (L) T cells of patients with COVID-19 or after recovery as compared to healthy controls. (**M**)
529 Heatmap showing color-coded relative levels of PD-1-targeting miR-138-5p, miR-15a-5p, miR-16-
530 5p and miR-28-5p miRNAs in $CD4^+$ and $CD8^+$ T cells of patients with COVID-19 and in those who
531 recovered from COVID-19 (n=10) normalized versus controls (n=5). **(N).** Bar graph comparing the
532 global immunological profiles of patients with COVID-19 after clinical symptom remission and
533 during the acute phase of the disease. Each bar depicts the proportion of patients for which the
534 value of the related factor is above the 75th percentile of the control group dataset. Data are
535 expressed as mean ± SEM. *$p<0.05$, **$p<0.01$; $^{\dagger}p<0.05$ as compared to healthy controls, calculated
536 with Kruskal-Wallis test (**B**, **D**, **F-H, K-L**) or two-sided unpaired t test (**I-J**, **M**).
537 **Abbreviations:** CTRL, healthy controls; COVID-19, patients with COVID-19; Post-COVID-19,
538 patients who recovered from COVID-19; LPS, lipopolysaccharide; DTaP, diphtheria-tetanus-
539 pertussis vaccine; FLU, flu vaccine; PBMCs, peripheral blood mononuclear cells; sPD-1, soluble
540 PD-1; sPD-L1, soluble PD-L1; FC, fold change; A.U., arbitrary units.

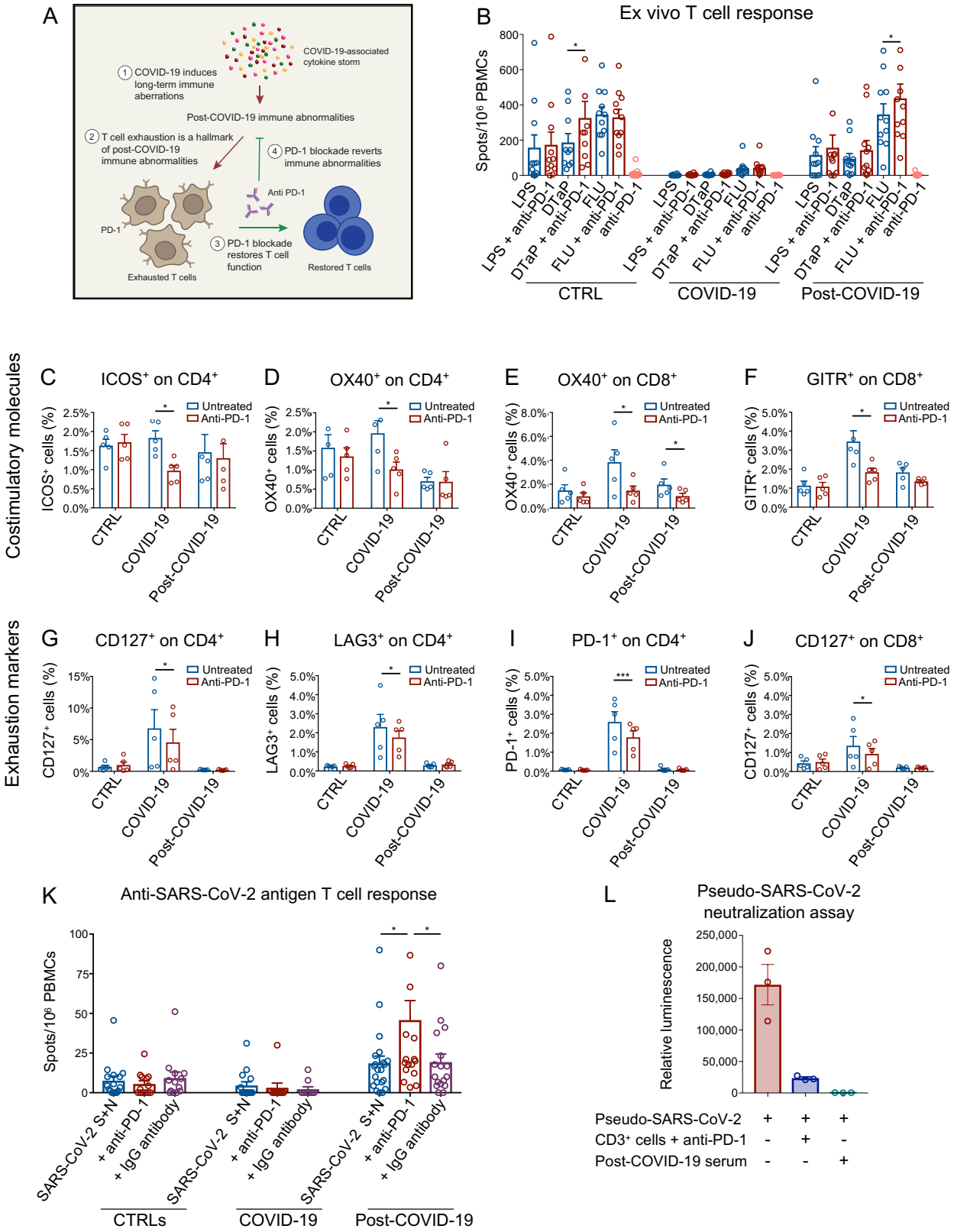

Figure 4. PD-1 blockade restores T cell function and the anti-SARS-CoV-2 antiviral T cell response in vitro. (A). Working hypothesis describing a PD-1 blockade-based strategy to reverse T cell exhaustion and restore the anti-SARS-CoV-2 immune response. **(B).** Bar graphs depicting the

545 effect of PD-1 blockade on the number of IFN-γ spots produced by ELISpot analysis of PBMCs
546 isolated from patients with COVID-19 (n=40), from those who recovered from COVID-19 (n=20)
547 and from healthy controls (n=35) following challenge with LPS, FLU, and DTaP, with or without
548 anti-PD-1 blocking antibody. **(C-J).** Effect of PD-1 blockade on the proportion of the costimulatory
549 markers ICOS and OX40 expressed by $CD4^+$ T cells, GITR and OX4 expressed by $CD8^+$ T cells
550 (**C-F**), exhaustion markers CD127, LAG3, PD-1 expressed by $CD4^+$ T cells, and CD127 expressed
551 by $CD8^+$ T cells (**G-J**) in PBMCs isolated from patients who recovered from COVID-19 (n=5)
552 cultured either alone or in the presence of anti-PD-1 bocking antibody. **(K).** Effect of PD-1
553 blockade on the number of IFN-γ spots by ELISpot analysis using PBMCs isolated from patients
554 with COVID-19 (n=40), from those who recovered from COVID-19 (n=20) and from healthy
555 controls (n=35) following challenge with spike and nucleocapsid SARS-CoV-2 peptides, with anti-
556 PD-1 bocking antibody or with anti-human IgG antibody. **(L).** Efficient T lymphocyte-dependent
557 neutralization of spike SARS-CoV-2 pseudotyped lentivirus by $CD3^+$ T cells following PD-1
558 blockade as assessed by luminescence-based neutralization assay (n=5). Serum of patients who
559 recovered from COVID-19 was used as control. Data are expressed as mean ± SEM. *$p<0.05$,
560 **$p<0.01$, ***$p<0.001$ calculated with two-sided paired t test (**B**, **C-J**) or one-way ANOVA (**K**, **L**).
561 **Abbreviations:** CTRL, healthy controls; COVID-19, patients with COVID-19; Post-COVID-19,
562 patients who recovered from COVID-19; PBMCs, peripheral blood mononuclear cells; LPS,
563 lipopolysaccharide; DTaP, diphtheria-tetanus-pertussis vaccine; FLU, flu vaccine; SARS-CoV-2
564 S+N, SARS-CoV-2 spike and nucleocapsid peptide pool.

565 **Tables**

566 **Table 1.** Baseline demographic and clinical characteristics of patients during hospitalization and of

567 healthy controls.

	CTRL (n=43)	*COVID-19 (n=57)*	*Post-COVID-19 (n=39)*	*p value*
Age, years	47.3 ± 2.1	54.7 ± 2.2	55.3 ± 2.4	ns
Male sex, n (%)	18 (41.9)	28 (49.1)	29 (74.4)[¥,§]	[†]p<0.001 [¥]p<0.01
Time from symptom onset, days	-	12.9 ± 1.3	137.6 ± 10.3	p<0.001
Time from discharge, days	-	-	102.9 ± 11.3	-
Coexisting conditions, n (%)	7 (16.3)	37 (66.1)	27 (69.2)	ns[A]
Diabetes, n (%)	0 (0.0)	16 (28.6)	5 (12.8)	ns[A]
Cardiovascular disease, n (%)	0 (0.0)	6 (10.7)	4 (10.3)	ns[A]
Hypertension, n (%)	3 (9.7)	19 (33.9)	17 (43.6)	ns[A]
Other, n (%)	4 (12,9)	30 (52.6)	18 (48.7)	ns[A]
Chronic treatment, n (%)	6 (14.0)	33 (66.2)	21 (56.8)	ns[A]
Antihypertensive drugs, n (%)	3 (9.7)	17 (32.1)	13 (35.1)	ns[A]
Glucose-lowering drugs, n (%)	0 (0.0)	11 (20.8)	4 (10.8)	ns[A]
Antithrombotic drugs, n (%)	0 (0.0)	13 (24.5)	4 (10.8)	ns[A]
Lipid-lowering drugs, n (%)	0 (0.0)	7 (13.2)	5 (13.5)	ns[A]
Others, n (%)	3 (9.7)	30 (53.6)	18 (46.1)	ns[A]
D-dimer (µg/mL)	-	3252 ± 2460	1850 ± 483	ns
CRP (mg/L)	-	70.0 ± 10.3	82.0 ± 14.7	ns
Major symptoms	-			
Fever, n (%)	-	48 (85.7%)	33 (91.7)	ns
Cough, n (%)	-	33 (58.9)	19 (52.8)	ns
Dyspnea, n (%)	-	21 (37.5)	12 (33.3)	ns
Diarrhea, n (%)	-	8 (14.3)	8 (22.2)	ns
Clinical score (0–7)	-	3.8 ± 0.1	3.9 ± 0.2	ns
Treatment during hospitalization	-			
Hydroxychloroquine, n (%)	-	29 (53.7)	30 (81.1)	p<0.05
Heparin, n (%)	-	29 (53.7)	13 (35.1)	ns
Anti-inflammatory, n (%)	-	54 (100)	26 (70.3)	p<0.001
Antiviral, n (%)	-	29 (53.7)	25 (67.6)	ns
Adverse events, n (%)	-	39 (68.4)	27 (67.5)	ns
Need for c-PAP, n (%)	-	10 (17.9)	17 (43.6)	p<0.05

Need for OTI, n (%)	-	6 (10.5)	4 (10.3)	ns
Oxygen therapy, n (%)	-	39 (68.4)	27 (69.2)	ns
ICU, n (%)	-	6 (10.5)	5 (12.8)	ns

(†): Post-COVID-19 vs. CTRL; (¥): Post-COVID-19 vs. COVID-19 calculated with Mann-Whitney or chi-square test; [A]Chi-square test performed between COVID-19 and Post-COVID-19

570 **Table 2.** $CD4^+$ and $CD8^+$ T cells positive for co-stimulatory and exhaustion markers.

	T cell population	*Marker*	*CTRL (n=15)*	*COVID-19 (n=30)*	*Post-COVID-19 (n=15)*	*p value*
Costimulatory molecules	$CD4^+$	$ICOS^+$ (%)	1.2 ± 0.2	2.4 ± 0.3§	2.0 ± 0.6	$^{\S}p<0.05$
		$OX40^+$ (%)	0.5 ± 0.1	0.8 ± 0.1§	0.5 ± 0.1	$^{\S}p<0.05$
		$CD40L^+$ (%)	0.8 ± 0.2	0.9 ± 0.1	0.5 ± 0.1$^{¥}$	$^{¥}p<0.05$
		$CTLA\text{-}4^+$ (%)	0.5 ± 0.1	0.6 ± 0.1	0.4 ± 0.0	ns
		$GITR^+$ (%)	1.2 ± 0.1	1.6 ± 0.1	1.7 ± 0.3	ns
	$CD8^+$	$ICOS^+$ (%)	0.6 ± 0.1	1.3 ± 0.2§	0.6 ± 0.1$^{¥}$	$^{\S}p<0.01$ $^{¥}p<0.05$
		$OX40^+$ (%)	0.3 ± 0.1	0.4 ± 0.1	0.5 ± 0.0†	$^{\dagger}p<0.05$
		$CD40L^+$ (%)	0.7 ± 0.1	0.8 ± 0.2	0.9 ± 0.1	ns
		$CTLA\text{-}4^+$ (%)	0.5 ± 0.1	0.5 ± 0.1	0.6 ± 0.1	ns
		$GITR^+$ (%)	1.1 ± 0.2	1.1 ± 0.1	1.4 ± 0.2$^{\dagger, ¥}$	$^{\dagger}p<0.01$ $^{¥}p<0.01$
Exhaustion markers	$CD8^+$	$CD127^+$ (%)	1.0 ± 0.1	1.5 ± 0.1§	1.8 ± 0.2†	$^{\S}p<0.05$ $^{\dagger}p<0.01$
		$PD\text{-}1^+$ (%)	0.9 ± 0.1	1.4 ± 0.2	1.4 ± 0.3	ns
		$2B4^+$ (%)	1.4 ± 0.2	1.2 ± 0.1	3.4 ± 0.4$^{\dagger, ¥}$	$^{\dagger}p<0.001$ $^{¥}p<0.001$
		$LAG3^+$ (%)	0.9 ± 0.2	0.7 ± 0.1	1.4 ± 0.2$^{¥}$	$^{¥}p<0.01$
		$TIGIT^+$ (%)	26.1 ± 1.9	25.9 ± 2.0	32.1 ± 2.3	ns

571 (§): COVID-19 vs. CTRL; (†): Post-COVID-19 vs. CTRL; (¥): Post-COVID-19 vs. COVID-19
572 calculated with Kruskal-Wallis test

573 **Table 3.** Long term clinical symptoms observed in patients who recovered from COVID-19.

Symptom	*Post-COVID-19 (n=39)*
Asthenia, n (%)	2 (5.1%)
Dyspnea, n (%)	12 (30.8%)
Tachypnea, n (%)	1 (2.6%)
Cough, n (%)	1 (2.6%)
Memory loss, n (%)	1 (2.6%)
Chest pain, n (%)	1 (2.6%)
Myalgia, n (%)	3 (7.7%)
Erythema, n (%)	2 (5.1%)
Nephropathy, n (%)	1 (2.6%)

574